Journal of Cerebral Blood Flow & Metabolism (2009) 29, 1175–1186

www.jcbfm.com

A new model of cortical stroke in the rhesus macaque

G Alexander West[1], Kiarash J Golshani[2,3], Kristian P Doyle[3], Nikola S Lessov[3], Theodore R Hobbs[4], Steven G Kohama[5], Martin M Pike[6], Christopher D Kroenke[5,6], Marjorie R Grafe[7], Maxwell D Spector[3], Eric T Tobar[3], Roger P Simon[8] and Mary P Stenzel-Poore[3]

[1]*Colorado Brain & Spine Institute, Neurotrauma Research Laboratory, Swedish Medical Center, Englewood, Colorado, USA;* [2]*Department of Neurosurgery, Oregon Health & Science University, Portland, Oregon, USA;* [3]*Department of Molecular Microbiology and Immunology, Oregon Health & Science University, Portland, Oregon, USA;* [4]*Division of Animal Resources, Oregon National Primate Research Center, Beaverton, Oregon, USA;* [5]*Division of Neuroscience, Oregon National Primate Research Center, Beaverton, Oregon, USA;* [6]*Advanced Imaging Research Center, Oregon Health & Science University, Portland, Oregon, USA;* [7]*Department of Pathology, Oregon Health & Science University, Portland, Oregon, USA;* [8]*Dow Neurobiology Laboratories, Legacy Good Samaritan Hospital, Portland, Oregon, USA*

Primate models are essential tools for translational research in stroke but are reportedly inconsistent in their ability to produce cortical infarcts of reproducible size. Here, we report a new stroke model using a transorbital, reversible, two-vessel occlusion approach in male rhesus macaques that produces consistent and reproducible cortical infarcts. The right middle cerebral artery (distal to the orbitofrontal branch) and both anterior cerebral arteries were occluded with vascular clips. Bilateral occlusion of the anterior cerebral artery was critical for reducing collateral flow to the ipsilateral cortex. Reversible ischemia was induced for 45, 60, or 90 mins ($n = 2$/timepoint) and infarct volume and neurologic outcome were evaluated. The infarcts were located predominantly in the cortex and increased in size with extended duration of ischemia determined by T_2-weighted magnetic resonance imaging . Infarct volume measured by 2,3,5-triphenyl tetrazolium chloride and cresyl violet staining corroborated magnetic resonance imaging results. Neurologic deficit scores worsened gradually with longer occlusion times. A subset of animals ($n = 5$) underwent 60 mins of ischemia resulting in consistent infarct volumes primarily located to the cortex that correlated well with neurologic deficit scores. This approach offers promise for evaluating therapeutic interventions in stroke.
Journal of Cerebral Blood Flow & Metabolism (2009) **29,** 1175–1186; doi:10.1038/jcbfm.2009.43; published online 22 April 2009

Keywords: cerebral ischemia; MRI; neurologic deficit; nonhuman primate; rhesus macaque; stroke

Introduction

Animal modeling is essential for the preclinical evaluation of neuroprotective drugs for the treatment of stroke. Rodent studies have provided substantial understanding of the pathophysiology of stroke and efficacy of interventions to protect the brain against ischemic injury (Gidday *et al*, 1999; Stenzel-Poore *et al*, 2007; Tamura *et al*, 1990). Additionally, the relative ease and efficiency of rodent models and their availability as inbred and genetically modified strains have led to comprehensive and successful stroke intervention studies, using an expanding array of molecular and pharmacologic agents (Huang *et al*, 1994; Liu *et al*, 2002). However, recent efforts to translate preclinical neuroprotective strategies from rodents to humans have been disappointing (Emerich, 2000; Savitz, 2007). There are numerous examples where promising neuroprotectants developed in rodent models have failed to reduce infarct size or improve functional outcome in humans. Moreover, some therapeutic trials in humans have actually led to increased mortality (Davis *et al*, 2000). Such discordance between rodent and human

Correspondence: Dr M Stenzel-Poore, Department of Molecular Microbiology and Immunology, L220, Oregon Health & Science University, 3181 Sam Jackson Park Road, Portland, OR 97239, USA.
E-mail: poorem@ohsu.edu
Received 24 November 2008; revised 6 March 2009; accepted 25 March 2009; published online 22 April 2009

responses to these therapeutic approaches may be due to species-specific differences in response to brain ischemia (DeGraba and Pettigrew, 2000; Grotta, 1995). Such considerations have led to the creation of STAIR guidelines (Stroke Therapy Academic Industry Round Table (Fisher M. Chair), 1999, 2005) and recent recommendations for preclinical testing of neuroprotective agents in nonhuman primates (NHPs) (Feuerstein *et al*, 2008).

The NHP models offer significant advantages for preclinical testing of candidate neuroprotective agents. Old-world monkeys, such as macaques and baboons, have a close phylogenetic relationship to humans, which increases the likelihood that these animals share similar endogenous mechanisms of ischemic injury and neuroprotection (Schmitz *et al*, 2005). Anatomically, most primate brains are much larger than rodent brains and possess gyrencephalic morphology and a gray/white matter ratio that is similar to that of humans. Critically, the anatomy of the cerebral vasculature in monkeys is analogous to humans (Kapoor *et al*, 2003), and thresholds for ischemia and infarction between monkeys and humans are very similar (Jones *et al*, 1981). The complex behavior of these animals also allows for a better assessment of functional outcome of after stroke recovery (Furuichi *et al*, 2007; Mack *et al*, 2003), which permits correlations of neurologic function with infarct size and location (Mack *et al*, 2003). Therefore, primate studies potentially offer an important translational bridge from rodents to humans by providing a pragmatic model in which to optimize the therapeutic drugs and their range of effectiveness while minimizing toxicity.

Primate models of stroke are quite varied, but frequently involve some aspects of occlusion (aneurysm clips, thrombus, embolization, etc.) of the middle cerebral artery (MCAO). To access this vessel, craniotomy has been used (Hirouchi *et al*, 2007), but this route is challenging because of the very thick overlying temporalis muscle and also the required brain retraction, which may result in mechanical injury to the brain. Hence, a transorbital approach to access the proximal intracerebral vessels (Spetzler *et al*, 1980) was used in this study. The results of MCAO, while promising (D'Arceuil *et al*, 2006; Furuichi *et al*, 2003; Kito *et al*, 2001; Maeda *et al*, 2005; Spetzler *et al*, 1980; Young *et al*, 1997), often produce infarcts that vary in location and size. Moreover, a long duration of ischemia is necessary to cause damage beyond the basal ganglia. Additional extended time of ischemia required for cortical involvement produces a mixture of cortical and subcortical stroke and can be associated with low survival. The resiliency of the monkey ipsilateral cortex to MCAO seems to be due to collateral flow to the region from the anterior cerebral arteries (ACAs), as occlusion of both ACAs and the internal carotid artery (ICA) in the baboon does induce cortical damage. However, in the ACA/ICA baboon model, the basal ganglia is also involved and heavily damaged; these animals frequently require extended postoperative care and may have significant morbidity and mortality (Huang *et al*, 2000; Mack *et al*, 2003). Moreover, reliance on occlusion of the ICA at the level of the anterior choroidal artery presents a technical challenge, due to lack of visualization of this artery and the proximity of the posterior communicating artery, which could result in persistent collateral flow through the posterior communicating artery.

Thus, current primate stroke models have not reliably produced large infarcts restricted to the cortex. Availability of such a model would mimic a subclass of thrombotic stroke in humans and offers a relatively homogenous therapeutic target for studies of neuroprotection. A model of cortical stroke would help address criticisms of the overly broad inclusion criteria in recent failed stroke trials, as stroke patients with either cortical or subcortical infarcts entered into these trials may have caused mixed results. This is illustrated in studies using the immunosuppressive agent FK506 in the NHP, which showed a significant reduction in infarct volume from MCAO, solely in the cortex and not in the basal ganglia (Furuichi *et al*, 2003, 2007). With long durations (hours) of ischemia, the cortical lesions often follow initial subcortical damage that progresses over time, creating secondary effects such as edema that can complicate interpretation of the effects of interventions.

The goals of this study are to create a reproducible cortical stroke model in the rhesus macaque and implement tools to evaluate damage as well as functional neurologic outcomes. Desirable features of this model are good survivability to evaluate therapeutic interventions and minimal postoperative care. Using a transorbital approach, reversible occlusion of the distal right middle cerebral and both ACAs produced reproducible infarcts that are located primarily in the cortex and that can serve as a relevant final screen for neuroprotective efficacy in the advancement of promising therapeutics for human clinical trials.

Materials and methods

Animals

Eleven adult, male rhesus macaques (*Macaca mulatta*), with an average age of 8.8 ± 0.6 years and an average body weight of 9.3 ± 0.5 kg, were selected for this study. Animals were singly housed indoors on a 12 h:12 h light/dark cycle, with lights-on from 0700 to 1900 h, and at a constant temperature of 24°C. Laboratory diet was provided twice daily, supplemented with fresh fruits and vegetables and drinking water *ad libitum*. Two weeks before surgery, animals were screened for general health, endemic diseases, and neurologic disorders, and blood was drawn for baseline evaluation of peripheral blood cell counts. All animal experiments were subject to approval and surveillance by the Institutional Animal Care and Use

Committee at the Oregon National Primate Research Center.

Experimental Design

Two experiments were conducted. An *Ischemia Duration Study* was performed to establish the optimal duration of ischemia necessary to generate a unilateral cortical infarct. An *Infarct Reproducibility Study* was performed to examine the reproducibility of stroke size and location after a specified duration of occlusion. The *Ischemia Duration Study* used 45, 60, and 90 mins ($n = 2$/group) occlusions and survival time of 7 days for the 45- and 60-min groups and 2 days for the 90-min group. The *Reproducibility Study* involved five animals given 60 mins of ischemia followed by a survival time of 2 days. Outcome measures (described below) for evaluating infarct size and neurologic changes were performed throughout the prescribed experimental recovery periods.

Two-Vessel Occlusion Protocol

Surgical procedures were conducted by a single surgeon to minimize variation. Anesthesia was induced with ketamine (10 mg/kg, intramuscular injection). Animals were then intubated and maintained under general anesthesia using 0.8% to 1.3% isoflurane vaporized in 100% oxygen. A blood sample was taken for a complete blood count and a venous line was placed for fluid replacement. An arterial line was established for blood pressure monitoring throughout surgery to maintain a mean arterial blood pressure of 60 to 80 mm Hg. End-tidal CO_2 and arterial blood gases were continuously monitored to titrate ventilation to achieve a goal of Pa_{CO_2} of 35 to 40 mm Hg.

Animals were positioned supine without a head-holding device. The right orbital area was clipped free of hair and cleaned with betadine. The medial and lateral canthi were incised as well as the periorbitum underneath the eyelids. The eye was exonerated and the optic nerve and its vessels were severed at the optic canal. The orbital roof was then drilled using a high-powered pneumatic drill and bone removed from the sphenoid wing, clinoid process, and medially to the planum sphenoidale. Using microdissection techniques under an operating stereomicroscope (Leica, Bannockburn, IL, USA) the dura was opened in a U-shaped manner with the base against the sphenoid wing and clinoid process. Removal of the medial border of the orbital roof and planum sphenoidale allowed direct access to the ICA, ACA, and MCA permitting reversible occlusion with aneurysm clips of the distal MCA and both ACAs (Figure 1). The MCA could be readily identified just anterior to the sphenoid wing. A titanium aneurysm mini-clip (Aesculap Inc., Center Valley, PA, USA) was placed on the MCA distal to the orbitofrontal artery, and a second aneurysm mini-clip was placed to occlude both ACAs proximal to the formation of a single pericallosal artery (Figure 1). After the occlusion period, mini-clips were removed, the cavity was irrigated, and periorbital fascia was placed over the dural opening to protect the brain surface. A large flat piece of bone wax was used to cover the bony opening and the eyelid was sutured closed.

Magnetic Resonance Imaging

All scans were performed on a Siemen's 3T Trio system, housed near the surgical suite at Oregon National Primate Research Center. Because of the small filling capacity of the rhesus macaque head, an extremity coil was used to achieve better image quality of the brain. For animals not already anesthetized, anesthesia was induced initially with ketamine (10 mg/kg, intramuscular injection). The animals were then intubated and administered 1% isofluorane vaporized in 100% oxygen for anesthesia maintenance. Animals were scanned in the supine position, and in most instances were scanned before surgery (baseline), immediately after surgery (acute), and 2 days after surgery. In the *Ischemia Duration Study*, four animals had a longer (7 day) period of recovery and were subjected to magnetic resonance imaging (MRI) scans during ischemia and also on day 2 and 7 of recovery. Animals were monitored for physiologic signs during scans, including pulse-oximetry, end-tidal CO_2, and respiration rate.

All animals received anatomical MRI scans, which included T_1- and T_2-weighted, high-resolution scans, and a diffusion-weighted scan. The T_1 scan was an MPRAGE protocol, with TR = 2500 ms, TE = 4.38 ms, number of averages = 1 and the flip angle = 12°. Full brain coverage was attained at a resolution of 0.5 mm isovoxel. The T_2 scan was a turbo spin-echo experiment, with TR = 5280 ms, TE = 57 ms, number of averages = 4, an echo train length of 5, and a refocusing pulse flip angle of 120° The entire brain was imaged with a 0.5×0.5 mm in-plane resolution and a slice thickness of 1 mm. For measurements of the directionally averaged water diffusion coefficient (the diffusion tensor trace/3), a turbo STEAM-based pulse sequence (Nolte *et al*, 2000) was used. With this strategy, image distortions typically encountered with standard echoplanar-imaging-based diffusion measurements within the NHP brain were avoided. The pulse sequence parameters were TR = 22000 ms, TE = 64 ms, and b = 900 s/mm^2. Full brain coverage was achieved with an in-plane resolution of 1.8×1.8 mm and a slice thickness of 2 mm.

Four of the animals from the *Ischemia Duration Study* that examined the effects of a variable duration of ischemia (45 and 60 min groups) were also scanned during the time the aneurysm clips were applied, to document perfusion in subregions of the brain. This information was obtained to establish the amount of intra-animal variation in the location of the infarct zone and the diminution of cerebral blood flow due to two-vessel occlusion. Dynamic susceptibility contrast-MRI, a bolus tracking perfusion MRI method, was used during the actual ischemic period to generate full brain maps of cerebral blood flow and volume. Ultrafast imaging requires an echoplanar-imaging sequence for dynamic susceptibility contrast-MRI and collects a rapid series of T_2^*-weighted images during administration of contrast (Prohance, 0.1 mmol/L/kg, i.v.). Full brain coverage yielded 20 slices at 1.5×1.5 mm in-plane, 2-mm slice thickness, with TR = 1500 ms and

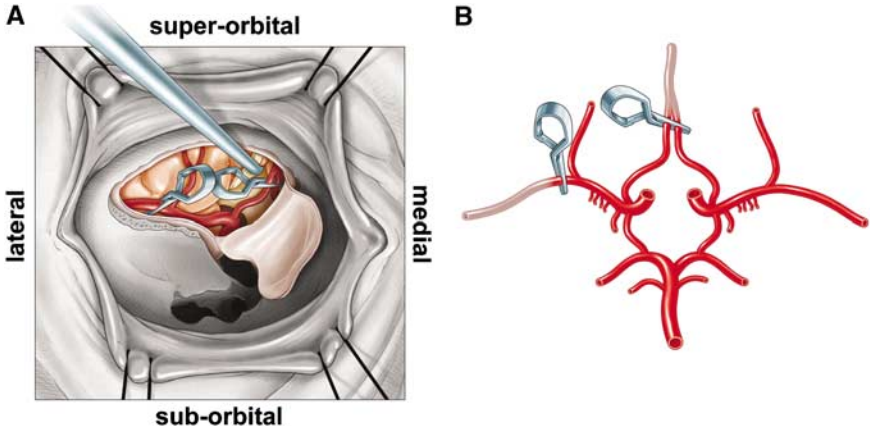

Figure 1 Schematic diagram of surgical site and vasculature of the rhesus two-vessel occlusion model. (**A**) *In situ* surgical view of the right orbit of the rhesus macaque illustrating the exposure of major cerebral arteries and positioning of aneurysm clips for occlusion of the right middle cerebral artery and bilateral anterior cerebral arteries. (**B**) *Ex vivo* illustration of the Circle of Willis with one clip on the middle cerebral artery distal to the orbitofrontal artery (lateral clip) and a second clip on both anterior cerebral arteries (medial clip) just before the vessels join to form a single pericallosal artery. 188 × 97 mm (400 × 400 DPI).

TE = 20 ms. Parametric maps were generated for cerebral blood flow (in ml blood/100 g tissue/minute), cerebral blood volume (in blood volume percentage of total tissue volume), and mean transit time (in seconds) using the JIM software package (Xinapse Systems, Thorpe Waterville, United Kingdom), following the model-independent method described by Ostergaard (2005). The arterial input function was determined from (approximately 20) brain pixels identified to have arterial input function characteristics (large, early, rapid intensity changes) by a two-stage automatic scanning and selection routine.

Neurologic Assessment

Neurologic assessment was performed on a daily basis by a single operator after stroke using a 100-point examination scale developed by Spetzler *et al* (1980). This scale evaluates motor function, behavior (mental status), and cranial nerve deficit. Higher scores represent better functional outcomes. Motor function is graded from 1 to 75, according to severity of hemiparesis in the extremities and face. Hemiparesis in the extremities is scored as 10 = severe hemiparesis, 25 = mild hemiparesis, 55 = favors normal side, or 70 = normal ability. Facial weakness is scored as 1 = one-sided paralysis and 5 = normal facial movement. Behavior and alertness are scored from 0 to 20, with 0 = dead, 1 = comatose, 5 = aware but inactive, 15 = aware but less active, and 20 = normal. Visual field deficits are scored as 1 when present or 5 when absent.

Tissue Collection

Animals were killed 2 days after stroke ($n = 7$) or 7 days after stroke ($n = 4$). Stroke subjects were sedated and then deeply anesthetized with 25 mg/kg sodium pentobarbitol. A blood sample was drawn for a complete blood count before exsanguination and perfusion with cold heparinized saline (2 U/mL) through the ascending aorta. Brains were rapidly removed, placed in a rhesus brain matrix (ASI, Warren, MI, USA) and cut into 15 consecutive, 4-mm thick coronal slabs per brain. For visualization of the region of infarction in a subset of animals, sections were immediately placed in 1.5% 2,3,5-triphenyl tetrazolium chloride (TTC, Sigma) in 0.9% phosphate-buffered saline and stained for 15 mins at 37°C. A further subset of animal brain sections was stained for 45 mins with TTC for increased infarct definition. After staining, sections were electronically imaged for subsequent analysis of infarct size and processed further for histology.

Histology and Histochemistry

Tissue slabs were fixed for 4 to 5 days in neutral-buffered 10% formalin containing increasing concentrations of sucrose (10% to 30%) for cryoprotection. To prevent freezing artifact, tissues were equilibrated at 4°C for 24 h in 10% glycerol and 2% dimethyl sulfoxide in 0.02 M potassium phosphate buffer (pH 7.4). This was followed by 3 to 4 days of immersion in 20% glycerol and 2% DMSO in 0.02 M potassium phosphate buffer (pH 7.4). After fixation and cryoprotection, the 4 mm slabs were frozen and then sectioned (30 to 50 μm) on a sliding microtome. The sections were mounted onto slides and one 50 μm section from each 4 mm slab was stained with cresyl violet for high magnification visualization of the infarcted area. These sections also served to determine the distribution of the injury between gray and white matter and the severity of the infarct within specific brain regions. In addition, representative slides with 30 μm sections were also processed for Fluoro-Jade B staining (Chemicon, Temecula, CA) as described by Schmued and Hopkins (2000) to identify damaged neurons.

Table 1 Physiological parameters and complete blood count (% differential) of animals in the *Infarct Reproducibility Study*

	Before occlusion	*During occlusion*	*Postocclusion*
Parameter			
Heart rate (b/min)	110.1 ± 5.5	124.7 ± 1.8	118.1 ± 9.0
Temp (°C)	98.3 ± 0.5	99.7 ± 0.3	99.8 ± 0.4
SpO_2	99.3 ± 0.5	98.7 ± 0.6	99.3 ± 0.4
$EtCO_2$ (mm Hg)	36.1 ± 1.6	36.5 ± 0.5	41.5 ± 4.8
Systolic blood pressure (mm Hg)	60.2 ± 3.7	67.0 ± 1.4	68.8 ± 2.3
Diastolic blood pressure (mmHg)	35.6 ± 1.2	38.7 ± 2.5	40.2 ± 2.6
% Differential			
Neutrophils	48.6 ± 6.4	N/D	69.0* ± 3.9
Lymphocytes	44.5 ± 5.6	N/D	23.7* ± 3.9
Monocytes	4.0 ± 0.6	N/D	8.0 ± 1.7
Eosinophils	2.0 ± 0.8	N/D	1.2 ± 0.2
Basophils	0.6 ± 0.9	N/D	0.6 ± 0.1

Stability of physiological parameters and white blood cell measurements were compared ($n = 5$; mean ± s.e.m.). *P-value < 0.05 compared with baseline samples. N/D, not done.

Infarct Measurements

Images from T_2-weighted MRIs, TTC, and cresyl violet-stained sections were examined for the location of infarction, and the total affected area was measured using NIH ImageJ v1.38 software (Bethesda, MD, USA). For the transverse slices of T_2-weighted image, measurement started from the level of the gyrus rectus. The brainstem and cerebellum in the inferior slices of the MRI were included in the hemispheric measurements. T_2 signal at the location of the surgical cavity was not included as part of the infarction, as this was due to the residual effects (fluid collection near the orbit) of the surgery. Each of the techniques (MRI, cresyl violet, TTC) used to measure infarct volume analyzed comparable anatomical regions and sampled approximately 15 slices (4 mm each). Measurements of infarct volume as a percentage of the ipsilateral hemisphere were made using the following formula: (area damaged/area of the ipsilateral hemisphere) × 100%. Total volume reflected calculations that compensated for slice thickness and intervening slices that were not directly measured. Basal ganglia involvement was specifically measured to compare the relative amount of damage versus the cortex.

Statistical Analysis

Experimental effects were analyzed using one-way analysis of variance, and in cases of significance, Bonferroni's post hoc test was used to determine pair-wise differences between treatment groups. Differences were considered statistically significant when $P < 0.05$. Error calculations for the Infarct Reproducibility study are presented in standard error of the mean, whereas calculations for the Duration of Ischemia study are presented in standard deviation as a result of small sample size. Correlations were prepared between pathologic and MRI stroke sizes, as well as infarct size and neurologic score using the square of the Pearson Product Moment Correlation Coefficient to generate R^2 values. Power analyzes were conducted using the online toolkit provided by DSS Research (www.dssresearch.com) with an α error of 5% and a β error of 25%.

Results

Intraoperative Monitoring and Hematology

The intraoperative vital signs and baseline hematological values for the five animals that underwent 60 mins of ischemia in the *Infarct Reproducibility Study* are provided in Table 1. There was no significant variation in vital signs measurements from baseline during ischemia and postocclusion values. There was also no evidence of hemorrhage or operative complications on the immediate postoperative MRI. However, after ischemia, there was a significant rise in the percentage of neutrophils and a significant reduction in lymphocytes. All animals survived for the preplanned 2 or 7 days of recovery, except one of the animals in the 90-min group. Animals given 60 mins of occlusion were capable of moderate self-care within 24 h. Self-care was confirmed when animals were capable of feeding, drinking, and self-grooming behaviors, although impaired due to the neurologic lesion. This outcome is desirable as it is consistent with similar neurologic assessments of humans who suffer cortical strokes.

Magnetic Resonance Imaging

Anatomical MRI scans of the animals revealed normal brain anatomy preischemia, as well as during the time period immediately after two-vessel occlusion (data not shown). At 2 days after stroke, T_2-weighted scans (Figure 2) closely matched the early lesion revealed by diffusion imaging, which retained a similar size and location at 2 days after stroke. The perfusion MRI (Figure 2A) revealed hypoperfusion that encompassed much of the

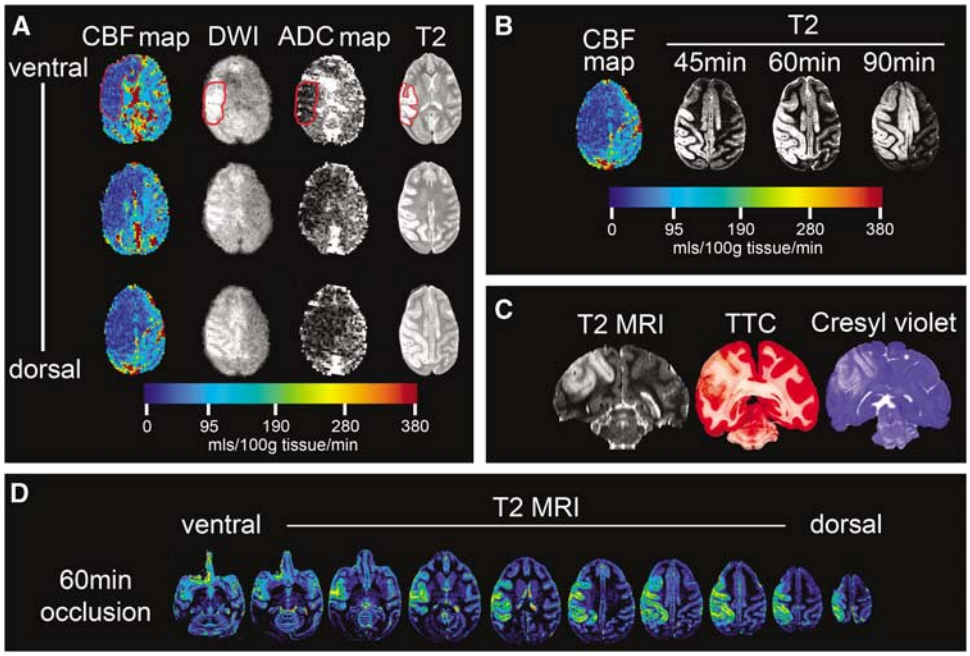

Figure 2 Development and distribution of ischemic damage after reversible, two-vessel occlusion. (**A**) Cerebral blood flow map, diffusion-weighted images (DWI), ADC maps, and T_2-weighted images are shown in three transverse slices taken from one animal. Cerebral blood flow, DWI, and ADC were obtained during occlusion and the T_2 scan was taken after 48 h. Hypoperfusion (dark blue) during 60 mins of ischemia resulted in smaller areas of subregional cortical damage (DWI and ADC) as verified with the T_2 scans. Regions of interest are encircled in red. (**B**) The effect of varying the duration of ischemia on the extent of cortical damage. The region of hypoperfusion is shown at one level in a typical example of a cerebral blood flow map and encompasses much of the ipsilateral hemisphere and some bilateral, midline structures. The amount of damage (T2 signal) at 48 h after ischemia increases with the duration of ischemia, encompassing more of the region that underwent hypoperfusion, including the bilateral cingulated gyrus. (**C**) Comparison of infarct damage after 60 mins occlusion using T_2-weighted MRI (48 h after ischemia), TTC, and cresyl violet-stained sections. There was excellent agreement in the amount of damage as assessed by the three different techniques. (**D**) Pseudo-colored distribution of damage is shown in transverse sections 2 days after 60 mins of reversible ischemia, by T_2-weighted MRI. Comprehensive cortical damage is evident throughout the brain on the side ipsilateral to the two-vessel occlusion. 279 × 190 mm (300 × 300 DPI).

ipsilateral hemisphere and some contralateral and midline structures immediately after the induction of stroke. The MRI scans obtained during ischemia were taken to clearly delineate the regions of the brain that were hypoperfused. These data allow the calculation of the infarct lesion volume based on the fraction of the perfusion deficit region or area at risk rather than the fraction of hemispheric volume. For the three animals scanned in this manner, the infarct lesion was 37 ± 2% of the area at risk and the average perfusion deficit region was 29 ± 3% of the total brain volume. Generally included within the perfusion deficit region were smaller enhanced regions in the diffusion-weighted images (DWI), also obtained during the occlusion period, and similar regions of hypointensity in the associated apparent diffusion coefficient maps created from them (Figure 2A). Hypoperfusion in the region of the cingulate cortex was observed, but this region was damaged bilaterally only after the more prolonged 90 mins duration of occlusion.

In the *Ischemia Duration Study*, the distribution of the infarct progressively enlarged as the duration of ischemia increased. After 60 mins of two-vessel occlusion, the infarct encompassed portions of the frontal, parietal, and insular motor cortex (Figure 2B), expanding with 90 mins of ischemia to include midline structures, such as the cingulate cortex. Anatomical T_2-weighted scans of animals with a longer survival time of 7 days (data not shown) showed expansion of the anomalous T_2-weighted image intensity beyond the original boundaries observed 2 days after ischemia. Despite the apparent diffusion of edema, the volume of infarct established using the T_2 MRI taken 2 days after stroke correlated well statistically (see below) with endpoint histology using TTC and cresyl violet (Figure 2C). Comprehensive cortical damage is evident throughout the ipsilateral hemisphere (Figure 2D).

Infarct Measurements: Correlation of MRI, TTC, and Cresyl Violet Techniques

To establish the best methodology for measuring infarct size, TTC-stained slices were compared with cresyl violet-stained sections as well as with

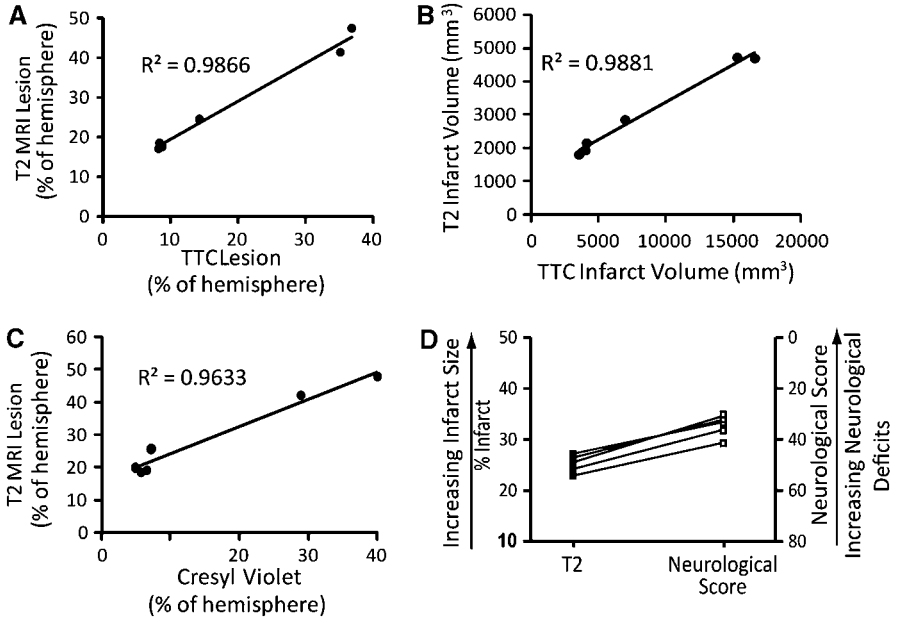

Figure 3 Correlation of primary outcome measures. (**A**–**C**) Animals were subjected to 45, 60, or 90 mins ($n = 2$/timepoint) of ischemia followed by 2 or 7 days of recovery. (**A**) Correlation of infarct measurement using T_2-weighted MRI versus TTC (percentage of hemisphere). (**B**) T_2 infarct volume (mm^3) versus TTC infarct volume (mm^3). (**C**) T_2-weighted MRI versus cresyl violet percentage of hemisphere. (**D**) Animals ($n = 5$) received 60 mins of ischemia followed by 2 days of recovery. Immediately before killing, animals underwent neurologic assessment followed by MRI scanning. Comparison of T_2-weighted MRI lesion measurements and neurologic score. 177 × 127 mm (300 × 300 DPI).

T_2-weighted MRI scans, obtained at day 2 or 7 after ischemia from animals in the *Ischemia Duration Study*. Stroke volume measured from T_2-weighted MRIs had a high R^2 of 0.9866 (as a % of the ipsilateral hemisphere) and 0.9881 (actual volume) when correlated to TTC-based estimates (Figures 3A and 3B). The correlation between infarct volumes measured by T_2-weighted MRI and cresyl violet-stained sections had an R^2 of 0.9633 (Figure 3C).

Duration of Ischemia

The effect of duration of reversible two-vessel occlusion on infarct size was examined in three groups of animals ($n = 2$/group) with occlusion times of 45, 60, or 90 mins. As expected, increasing the duration of ischemia resulted in larger cortical infarct size (Table 2), with additional expansion into midline structures in hypoperfused regions defined by perfusion MRI. The associated neurologic scores generally, but not absolutely, reflected increased damage with lower (worse) scores. The animals with 45 mins occlusions had a mean infarct volume of $1982.5 \pm 251\,mm^3$, which involved a mean of $19.0 \pm 0.98\%$ of the ipsilateral hemisphere based on T_2-weighted MRI. There was no noticeable damage to the basal ganglia; the average neurologic score at 48 h after stroke was 34.5 ± 4.9 (Table 2).

Animals with 60-min occlusions had a mean infarct volume of $2381 \pm 654\,mm^3$, which involved a mean infarct size of $22.1 \pm 4.6\%$ of the ipsilateral hemisphere based on T_2-weighted MRI. Damage to the basal ganglia continued to be very small and was not observed in all animals. The average neurologic score at 48 h was 30.5 ± 0.7 (Table 2).

The 90-min occlusion involved a greater portion of the cortex and resulted in the death of one of the animals before day 2 after stroke scan. Post mortem T_1-, T_2-, and diffusion-weighted scans all revealed extensive ipsilateral damage that resulted in a slight midline shift of the brain (data not shown), similar to the other animal in this group. As assessed by T_2-weighted MRI, the mean infarct volume was $4707 \pm 12.7\,mm^3$, which was $44.4 \pm 4.0\%$ of the ipsilateral hemisphere. Cresyl violet measurement of the mean infarct size was $34.4 \pm 7.8\%$ of the ipsilateral hemisphere. Unlike the shorter 45 or 60 mins of ischemia, 90 mins of stroke resulted in minor basal ganglia involvement of 4.1% of the ipsilateral hemisphere. The mean neurologic score at 24 h was 26 ± 1.4. The surviving animal had a neurologic score of 27 at 48 h after stroke (Table 2, animal #5).

Infarct Reproducibility

A duration of 60 mins of ischemia resulted in moderate-sized infarcts, good survivability, and obvious neurologic effects in the *Ischemia Duration Study*; thus, we selected this duration of ischemia for the *Infarct Reproducibility Study* (Table 2, animals #7 to 11). T_2-weighted MRI scans and cresyl violet

Table 2 Summary of primary outcome measurements

				% ipsilateral hemisphere infracted			% ipsilateral cortex infarcted	Infarct volume	Neurological Score (48 h postocclusion)		
Study	*#*	*Ischemia (min)*	*Survival (days)*	*TTC*	*T2 MRI*	*Cresyl violet*	*T2 MRI*	*T2 MRI (mm^3)*	*Motor function*	*Behavior and alertness*	*Total score*
Ischemia duration	1	45	7	8.6	18.3	21.53	N/D	1805	23	15	38
	2	45	7	8.7	19.7	28.84	N/D	2160	19	12	31
	3	60	7	9.1	18.9	25.25	N/D	1918	21	10	31
	4	60	7	14.4	25.4	26.88	N/D	2844	20	10	30
	5	90	2	36.4[a]	47.3	39.9	N/D	4716	15	12	27
	6	90	2	34.8[a]	41.6	28.9	N/D	4698	N/D	N/D	N/D
Infarct reproducibility	7	60	2	21.1[a]	23.3	21.1	42.5	2558	23	18	41
	8	60	2	23.2[a]	24.2	26.9	39.5	2664	20	16	36
	9	60	2	23.0[a]	27.0	25.0	47.0	2980	20	13	33
	10	60	2	31.7	25.7	24.3	43.6	3699	18	13	31
	11	60	2	30.0	26.6	23.3	35.1	2269	20	12	32

Ischemia Duration Study (rhesus #1–6) and Infarct Reproducibility Study (rhesus #7–11).
[a]Measurements from brain slices stained with TTC for 45 mins. All other slices stained with TTC for 15 min. N/D, not done.

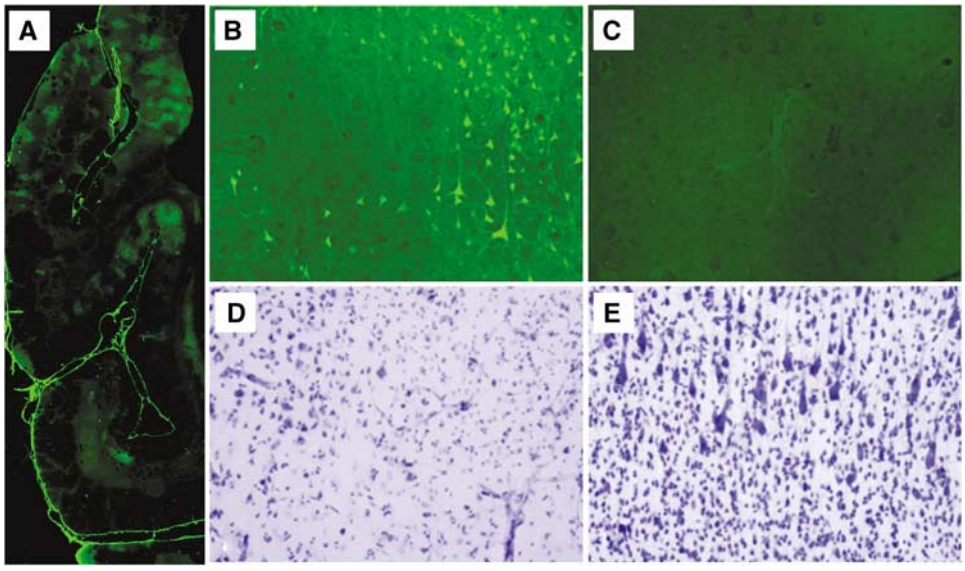

Figure 4 Histologic evidence of moderate to severe cortical injury after 60 mins occlusion. (**A**) Low magnification montage of infarct (Fluoro-Jade B; green label) predominantly restricted to the cortical ribbon. (**B**) and (**D**) show an area of fronto-parietal cortex with a patchy, discontinuous region of injury. In (**B**), the bright, Fluoro-Jade B-labeled neurons have suffered ischemic damage, and unaffected, unstained neurons are darker than the background neuropil. A Nissl-stained adjacent section (**D**) shows the residual intact neurons (left) versus the right side of the figure, which shows loss of neurons and prominent capillaries. (**C**) and (**E**) show uninjured contralateral fronto-parietal cortex. No Fluoro-Jade B neurons are seen in (**C**) and normal cortical architecture and neuronal staining are observed in (**E**). 241 × 141 mm (300 × 300 DPI).

staining revealed a similar cortical pattern of damage as described above, with little (approximately 1%) basal ganglia involvement. The amount of infarcted cortical gray matter measured from T_2-weighted MRI scans was $2834 \pm 244\,mm^3$, or $41.5 \pm 2.0\%$ of the ipsilateral cortex. This amount of damage was equal to $25.4 \pm 0.7\%$ of the ipsilateral hemisphere, very similar to cresyl violet ($24.1 \pm 0.9\%$) and TTC ($25.8 \pm 2.1\%$) measurements. Neurologic deficits were moderate with a marked hemiparesis on the affected side and a total score at 48 h after stroke of 34.6 ± 1.8. Neurologic scoring and final infarct size revealed a consistent relationship (Figure 3D). A power analysis of the seven animals that received

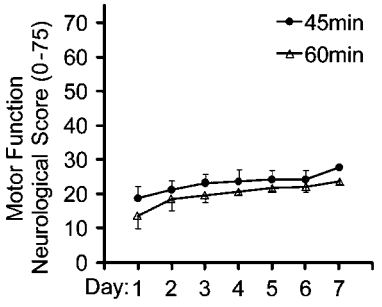

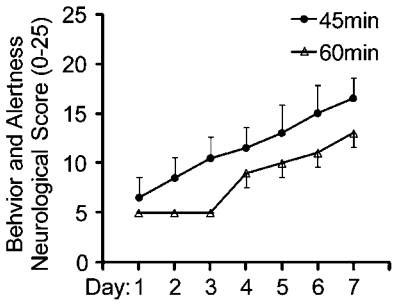

Animal #	Ischemia (min)	Day 1	2	3	4	5	6	7
1	45	21	23	25	26	26	26	28
2	45	16	19	21	21	22	22	27
3	60	16	21	21	21	22	23	24
4	60	11	16	18	20	21	21	23

Animal #	Ischemia (min)	Day 1	2	3	4	5	6	7
1	45	8	10	12	13	15	17	18
2	45	5	7	9	10	11	13	15
3	60	5	5	5	10	11	12	14
4	60	5	5	5	8	9	10	12

Figure 5 Motor and behavioral improvement over 7 days after occlusion. Animals were evaluated daily for 7 days after 45 min ($n = 2$) or 60 min ($n = 2$) occlusion. Evaluations consisted of neurologic assessments as described in Materials and methods. Analgesics were discontinued 24 h after surgery and animals were scored daily. 179 × 106 mm (300 × 300 DPI).

60 mins of occlusion revealed that an N of 6 would be required to find a 15% or greater reduction in infarct size statistically significant.

Histology

Histopathologic evaluation of Fluoro-Jade B and cresyl violet-stained specimens revealed that the portions of the frontal, parietal, somatosensory, and the insular cortex were consistently injured in all animals subjected to 60 mins of reversible two-vessel occlusion. Subcortical white matter injury was minor and proximal to cortical injury; no injury to deep white matter tracts was observed microscopically. The superior temporal gyrus and the basal ganglia were inconsistently injured. Representative Fluoro-Jade B and cresyl violet images showing neuronal injury in the ipsilateral cortex are provided in Figure 4. Animals with 60 mins occlusions had discontinuous patches of gray matter injury, while animals that underwent 90 mins occlusions had more confluent injury. In addition, 90 mins occlusions extended injury to midline structures in the ACA distribution, such as the cingulate and anterior frontal cortex, as described in T_2-weighed MRI scans.

Extended Survival

Four animals from the *Ischemia Duration Study*, two from the 45 mins occlusion, and two from the 60 mins occlusion were scored neurologically each day for 7 days after occlusion. This allowed evaluation of neurologic deficits in the absence of the potentially confounding effects of analgesics commonly used immediately after surgery. All animals showed a steady improvement in behavior and motor function over 7 days (Figure 5). The difference between animals receiving 45 mins versus 60 mins of occlusion shows the potential ability to recognize the attenuation of neurologic deficits in animals in a preclinical trial. The rate of recovery was attenuated for animals undergoing the longer stroke period of vascular occlusion. Also, there was sufficient room for improvement of the neurologic scores suggesting that successful interventions would not be inhibited by a ceiling effect. This pattern of behavioral and motor recovery is consistent with observations from clinical stroke patients (Traversa *et al*, 2000).

Discussion

The ideal method for stroke modeling in the primate is uncertain. Although the MCAO offers significant advantages, previous NHP studies had limited success in producing reproducible cortical infarcts. MCAO in the baboon produced significant, but variably sized strokes located primarily in the basal ganglia (Del Zoppo *et al*, 1986). A transorbital approach in baboons that used clips on the proximal MCA and the orbitofrontal branch of the MCA produced no infarction in six animals, and only a limited basal ganglia infarction in another six animals after 6 h of occlusion (Young *et al*, 1997). A similar approach in cynomolgus monkeys produced larger infarcts about 1000 mm^3 in size after 3 h of occlusion, but infarcts were primarily localized to the basal ganglia (Takamatsu *et al*, 2000). Ninety minutes MCA only occlusion in the rhesus produced infarcts that were primarily located in the caudate and also varied in size (Murphy *et al*, 2008). Thus, these approaches do not fully mimic the clinical situation of cortical stroke.

An alternative model of stroke uses thrombosis to create occlusion. However, one study of thromboem-

bolic occlusion of the ICA in cynomolgus monkeys still results in a significantly variable infarct primarily located in the basal ganglia (Kito *et al*, 2001). Thrombosis of the MCA, induced by activating intravascular rose bengal with photoirradiation (Maeda *et al*, 2005) also produced significant variability in infarct size. A PET scan performed during the ischemic induction showed cyclic flow reductions in the brain likely related to thrombus formation and embolization more distally. Therefore, we opted for the use of aneurysm clips for better control of placement, completeness, and reversibility of occlusion.

To develop a model of cortical stroke in the rhesus macaque, we initially performed a pilot study with different durations of reversible proximal MCA (single-vessel) trunk occlusion. MCAO ranging from 3 to 6 h resulted in progressively larger basal ganglia damage, but with little cortical involvement (data not shown). Four hours of occlusion of the orbitofrontal branch and the proximal trunk of the MCA also caused infarcts that were modest and localized to the basal ganglia (data not shown), suggesting sufficient collateral flow protected the cortex. Occlusion of both ACAs and one ICA in the baboon was reported to create a mixed stroke involving both the basal ganglia and cortex (Huang *et al*, 2000), but with significant morbidity and mortality. The occlusion of the ICA at the level of the anterior choroidal artery can also be challenging, where lack of visualization and proximity of the posterior communicating artery could result in persistent collateral flow through the posterior communicating artery. These data along with our experience suggesting a significant amount of collateral flow in the rhesus macaque, using the two-vessel occlusion approach to include the MCA (distal to the orbitofrontal and lenticulostriate arteries) and bilateral occlusion of ACAs would preserve the basal ganglia while establishing ischemia in the cortex.

There are apparent species differences on how ICA and/or MCA occlusion affects the evolution of stroke in humans versus macaques. The two proximal (A1) ACAs in the macaque merge to form the single (A2) pericallosal artery (Kapoor *et al*, 2003), which supplies both hemispheres (Coceani *et al*, 1966). While humans may also have cross-filling of the contralateral A2 through the ACA, collateral supply is variable and often limited by the small size of the ACA. Hence, strokes in humans by ICA occlusion or downstream ipsilateral MCA involvement alone can result in cortical lesions, while it is plausible that collateral flow in the macaque ACAs can provide significantly more cortical protection.

To maximize cortical infarction and minimize basal ganglia involvement and variability, we combined occlusion of the MCA (with preservation of blood flow in the orbitofrontal artery and lenticulostriate arteries) with the elimination of collateral circulation through the ACAs. We were able to show a close correlation of neurologic deficits and infarct sizes measured by T_2-weighted MRI, TTC, and cresyl violet staining in our model, similar to others (Huang *et al*, 2000; Mack *et al*, 2003). Damage to the cortex correlated with duration of ischemia and was directly related to neurologic outcome. Although the bilateral ACA occlusion in this model is not directly translatable to human MCAO stroke, titrating the duration of the vascular occlusion, we avoided bilateral damage and contralateral edema.

In the peripheral blood, stroke resulted in an elevation in the neutrophil count and a significant reduction in the lymphocyte count analogous to findings in humans stroke, which may be a prognostic indicator (Clark *et al*, 1996; Kasner *et al*, 2001; Ross *et al*, 2007). Murphy *et al* also found neutrophil and macrophage infiltrates on the borders of their lesions (Murphy *et al*, 2008). These are stroke-induced changes that may point to interventions in immunologic function that could modulate after stroke effects.

The use of diffusion-weighted MRI in our model allowed identification of an ischemic core region, indicating metabolically stressed areas at high risk of proceeding to infarction. Areas outside these regions that are within the perfusion deficit region can be considered the ischemic penumbra, which in this model, as in clinical settings, is largely salvaged by reperfusion. However, the ischemic core, which generally expands toward the boundaries of the perfusion deficit region with increased duration of ischemia, is the primary target region for neuroprotection. Generally, the pattern and scope of the DWI changes during ischemia were similar to T_2-weighted images of cortical edema at 48 h after stroke in these nontreated animals, but it is likely that a comparison with treated animals would reveal portions of the ischemic core that have been spared injury by antecedent therapy such as preconditioning. The timing of the collection of MRI specifically during this acute postischemic period may be particularly important. Other studies have observed that the affected volume, as seen by MRI (T_2-weighted, diffusion-weighted, or fluid-attenuated inversion recovery (FLAIR)) peaks 1 to 3 days after reversible ischemia match the final infarct size, has been reported earlier in monkeys (D'Arceuil *et al*, 2006; Liu *et al*, 2007) and rodents (Li *et al*, 2000; Sotak, 2002). Thus, MRI in this timeframe can be an important tool for assessing the evolution and extent of infarct, as well as the effect of neuroprotection, as some tissue should be salvageable by successful treatment in the regions of hypoperfusion.

Thus, transient occlusion of the MCA and bilateral ACAs in the rhesus macaque produces reproducible, clinically relevant, cortical infarcts with limited variability between MRI and histologic measures and results in excellent survival. In addition, neurologic deficits correlate well with levels of damage and subcortical (basal ganglia) injury is minimized. Because of the fact that the deep white matter is largely intact, preservation of penumberal areas of

cortex by a neuroprotectant is likely to be apparent clinically. With a moderate cortical infarct volume of approximately 25%, this model provides latitude for modulating infarct size to test the negative or positive effects of candidate therapeutics. Assessment of putative therapeutics in such a NHP stroke model may reduce the frequency of failed human clinical trials and offers the potential for preclinical screening of neuroprotective agents aimed at reducing cortical infarction in large-vessel stroke in humans.

Acknowledgements

The authors acknowledge support from the Oregon Health & Science Bioscience Innovation Fund, National Institute of Health, NINDS NS050567 (MSP), NS35965 (RPS), the National Institute of Health, NINDS NS043997 (GAW), and The National Center for Research Resources RR-00163 (SGK).

References

Clark WM, Hazel JS, Beamer N, Wynn M, Coull B (1996) The initial acute phase response predicts long term stroke recovery. *Stroke (Abstract)* 7:128–31

Coceani F, Libman I, Gloor P (1966) The effect of intracarotid amobarbital injections upon experimentally induced epileptiform activity. *Clin Electroencephalogr* 20:542–58

D'Arceuil HE, Duggan M, He J, Pryor J, de Crespigny A (2006) Middle cerebral artery occlusion in Macaca fascicularis: acute and chronic stroke evolution. *J Med Primatol* 35:78–86

Davis SM, Lees KR, Albers GW, Diener HC, Markabi S, Karlsson G, Norris J (2000) Selfotel in acute ischemic stroke: possible neurotoxic effects of an NMDA antagonist. *Stroke* 31:347–54

DeGraba T, Pettigrew L (2000) Why do neuroprotective drugs work in animals but not humans? *Neurol Clin* 18:475–93

Del Zoppo GJ, Copeland BR, Harker LA, Waltz TA, Zyroff J, Hanson SR, Battenberg E (1986) Experimental acute thrombotic stroke in baboons. *Stroke* 17:1254–65

Emerich DF (2000) Clinical trials with neuroprotective drugs in acute ischaemic stroke: are we doing the right thing? *Trends Neurosci* 23:245–6

Feuerstein GZ, Zaleska MM, Krams M, Wang X, Day M, Rutkowski JL, Finklestein SP, Pangalos MN, Poole M, Stiles GL, Ruffolo RR, Walsh FL (2008) Missing steps in the STAIR case: a translational medicine perspective on the development of NXY-059 for treatment of acute ischemic stroke. *J Cereb Blood Flow Metab* 28:217–9

Furuichi Y, Maeda M, Matsuoka N, Mutoh S, Yanagihara T (2007) Therapeutic time window of tacrolimus (FK506) in a nonhuman primate stroke model: comparison with tissue plasminogen activator. *Exp Neurol* 204:138–46

Furuichi Y, Maeda M, Moriguchi A, Sawamoto T, Kawamura A, Matsuoka N, Mutoh S, Yanagihara T (2003) Tacrolimus, a potential neuroprotective agent, ameliorates ischemic brain damage and neurologic deficits after focal cerebral ischemia in nonhuman primates. *J Cereb Blood Flow Metab* 23:1183–94

Gidday J, Shah A, Mceren R, Wang Q, Pelligrino D, Holtzman D, Park T (1999) Nitric oxide mediates cerebral ischemic tolerance in a neonatal rat model of hypoxic preconditioning. *J Cereb Blood Flow Metab* 19:331–40

Grotta J (1995) Why do all drugs work in animals but none in stroke patients? 2. Neuroprotective therapy. *J Intern Med* 237:89–94

Hirouchi Y, Suzuki E, Mitsuoka C, Jin H, Kitajima S, Kohjimoto Y, Enomoto M, Kugino K (2007) Neuroimaging and histopathological evaluation of delayed neurological damage produced by artificial occlusion of the middle cerebral artery in Cynomolgus monkeys: establishment of a monkey model for delayed cerebral ischemia. *Exp Toxicol Pathol* 59:9–16

Huang J, Mocco J, Choudhri TF, Poisik A, Popilskis SJ, Emerson R, DelaPaz RL, Khandji AG, Pinsky DJ, Connolly Jr ES (2000) A modified transorbital baboon model of reperfused stroke. *Stroke* 31:3054–63

Huang Z, Huang PL, Fishman MC, Moskowitz MA (1994) Effects of cerebral ischemia in mice deficient in neuronal nitirc oxide synthase. *Science* 265:1883–5

Jones TH, Morawetz RB, Crowell RM, Marcoux FW, FitzGibbon SJ, DeGirolami U, Ojemann RG (1981) Thresholds of focal cerebral ischemia in awake monkeys. *J Neurosurg* 54:773–82

Kapoor K, Kak VK, Singh B (2003) Morphology and comparative anatomy of circulus arteriosus cerebri in mammals. *Anat Histol Embryol* 32:347–55

Kasner SE, Demchuk AM, Berrouschot J, Schmutzhard E, Harms L, Verro P, Chalela JA, Abbur R, McGrade H, Christou I, Krieger DW (2001) Predictors of fatal brain edema in massive hemispheric ischemic stroke. *Stroke* 32:2117–23

Kito G, Nishimura A, Susumu T, Nagata R, Kuge Y, Yokota C, Minematsu K (2001) Experimental thromboembolic stroke in cynomolgus monkey. *J Neurosci Methods* 105:45–53

Li F, Liu KF, Silva MD, Omae T, Sotak CH, Fenstermacher JD, Fisher M, Hsu CY, Lin W (2000) Transient and permanent resolution of ischemic lesions on diffusion-weighted imaging after brief periods of focal ischemia in rats: correlation with histopathology. *Stroke* 31: 946–54

Liu H, Xin L, Chan BPL, Teoh R, Tang BL, Tan YH (2002) Interferon beta administration confers a beneficial outcome in a rabbit model of thromboembolic cerebral ischemia. *Neurosci Lett* 327:146–8

Liu Y, D'Arceuil HE, Westmoreland S, He J, Duggan M, Gonzalez RG, Pryor J, de Crespigny AJ (2007) Serial diffusion tensor MRI after transient and permanent cerebral ischemia in nonhuman primates. *Stroke* 38:138–45

Mack WJ, Komotar RJ, Mocco J, Coon AL, Hoh DJ, King RG, Ducruet AF, Ransom ER, Oppermann M, DeLaPaz R, Connolly Jr ES (2003) Serial magnetic resonance imaging in experimental primate stroke: validation of MRI for pre-clinical cerebroprotective trials. *Neurol Res* 25:846–52

Maeda M, Takamatsu H, Furuichi Y, Noda A, Awaga Y, Tatsumi M, Yamamoto M, Ichise R, Nishimura S, Matsuoka N (2005) Characterization of a novel thrombotic middle cerebral artery occlusion model in monkeys that exhibits progressive hypoperfusion and robust cortical infarction. *J Neurosci Methods* 146:106–15

Murphy SJ, Kirsch JR, Zhang W, Grafe MR, West GA, del Zoppo GJ, Traystman RJ, Hum PD (2008) Can gender

differences be evaluated in a rhesus macaque (Macaca mulatta) model of focal cerebral ischemia? *Comp Med* 58:588–96

Nolte UG, Finsterbusch J, Frahm J (2000) Rapid isotropic diffusion mapping without susceptibility artifacts: whole brain studies using diffusion-weighted single-shot STEAM MR imaging. *Magn Reson Med* 44:731–6

Ostergaard L (2005) Principles of cerebral perfusion imaging by bolus tracking. *J Magn Reson Imaging* 22:710–7

Ross AM, Hurn P, Perrin N, Wood L, Carlini W, Potempa K (2007) Evidence of the peripheral inflammatory response in patients with transient ischemic attack. *J Stroke Cerebrovasc Dis* 16:203–7

Savitz SI (2007) A critical appraisal of the NXY-059 neuroprotection studies for acute stroke: a need for more rigorous testing of neuroprotective agents in animal models of stroke. *Exp Neurol* 205:20–5

Schmitz J, Roos C, Zischler H (2005) Primate phylogeny: molecular evidence from retroposons. *Cytogenet Genome Res* 108:26–37

Schmued LC, Hopkins KJ (2000) Fluoro-Jade B: a high affinity fluorescent marker for the localization of neuronal degeneration. *Brain Res* 874:123–30

Sotak CH (2002) The role of diffusion tensor imaging in the evaluation of ischemic brain injury—a review. *NMR Biomed* 15:561–9

Spetzler RF, Selman WR, Weinstein P, Townsend J, Mehdorn M, Telles D, Crumrine RC, Macko R (1980) Chronic reversible cerebral ischemia: evaluation of a new baboon model. *Neurosurgery* 7:257–61

Stenzel-Poore MP, Stevens SL, King JS, Simon RP (2007) Preconditioning reprograms the response to ischemic injury and primes the emergence of unique endogenous neuroprotective phenotypes: a speculative synthesis. *Stroke* 38:680–5

Stroke Therapy Academic Industry Round Table (Fisher M. Chair) (1999) Recommendations for standards regarding preclinical neuroprotective and restorative drug development. *Stroke* 30:2752–8

Stroke Therapy Academic Industry Round Table (Fisher M. Chair) (2005) Enhancing the development and approval of acute stroke therapies: Stroke Therapy Academic Industry roundtable. *Stroke* 36:1808–13

Takamatsu H, Tsukada H, Kakiuchi T, Nishiyama S, Noda A, Umemura K (2000) Detection of reperfusion injury using PET in a monkey model of cerebral ischemia. *J Nucl Med* 41:1409–16

Tamura A, Kirino T, Sano K, Takagi K, Oka H (1990) Atrophy of the ipsilateral substantia nigra following middle cerebral artery occlusion in the rat. *Brain Res* 510:154–7

Traversa R, Cicinelli P, Oliveri M, Giuseppina Palmieri M, Filippi MM, Pasqualetti P, Rossini PM (2000) Neurophysiological follow-up of motor cortical output in stroke patients. *Clin Neurophysiol* 111:1695–703

Young AR, Touzani O, Derlon JM, Sette G, MacKenzie ET, Baron JC (1997) Early reperfusion in the anesthetized baboon reduces brain damage following middle cerebral artery occlusion: a quantitative analysis of infarction volume. *Stroke* 28:632–8